HiSST: 3rd International Conference on
High-Speed Vehicle Science Technology
14 -19 April 2024, Busan, Korea

Study on Equal-Intensity-Distribution Configuration of External-Compression Multi-Wave Curved-Shock Flowfields

Wenguo Luo[1], Changkai Hao[2], Jianfeng Zhu[3], Yancheng You[4]

Abstract

In this paper, based on the computational principle of the inverse method of characteristic, an inverse design method that can specify the compression process of the two-dimensional/axisymmetric captured flow tube is developed for the external-compression multi-wave flowfield of curved surface compression. On this basis, it is proposed that a kind of configuration for curved shock system with the same intensity distribution in the capture height direction. An index parameter named surface compression efficiency ratio is introduced to measure the performance of the equal-intensity-distribution flowfield. The both characteristics of the total pressure recovery and the compression efficiency in the cases of different shock numbers are emphatically studied. In addition, the compression limit of curved shock system is discussed when the initial shock wave is given in different function forms. The results show that the multi-wave flow field with Equal-Intensity-Distribution configuration is actually determined by the initial shock. Enhancing the curved compression characteristics of the initial shock, rather than adding one or two shock waves, could be possible to achieve a total pressure recovery equivalent to or even better than that of the straight shock system, so as to simplify the flowfield wave system. For the initial shock wave in the form of convex function, compared with one end of the focused shocks, the smaller the shock curvature at the other end away from the shock focal point, the higher total pressure recovery that the compression limit could reach.

Keywords: *Multi-wave curved compression, Inverse method of characteristic, Equal-intensity-distribution curved-shock configuration.*

1. Introduction

The organization of supersonic shock wave system is a key basic problem in the aerodynamic design[1-3]. In the flight process through wide speed range and large airspace, the great change of wave system configuration will become the most distinctive physical features of inlet flow field evolution.

In order to design the inlet aerodynamic surface with high compression efficiency under the condition of wide speed range, it is of great basic significance to carry out the research on the configurations of compression wave system. In recent years, the flowfield configuration of curved shock compression has been proved to have the advantages of high compression efficiency and controllable shock compression/isentropic compression ratio, so it has been widely concerned in the field of supersonic and hypersonic flow research.

The design of curved-shock compression surface could adopt the forward design of directly giving wall coordinates [4] or the inverse design based on Prandtl-Meyer equation[5-6]. While the inverse design method based on the method of characteristic (MOC) [7] has been widely used because of its simplicity, accuracy and wide adaptability, and has developed many ways to realize the flowfield calculation, such as based on given wall aerodynamic parameters [8-11], based on downstream section aerodynamic parameters [12-13], based on shock shapes [14] and so on. However, these flowfield calculation

[1] *School of Aerospace Engineering, Xiamen University, China, 35020200156008@stu.xmu.edu.cn*
[2] *School of Aerospace Engineering, Xiamen University, China, haochangkai@stu.xmu.edu.cn*
[3] *School of Aerospace Engineering, Xiamen University, China, zhjf@xmu.edu.cn (Corresponding Author)*
[4] *School of Aerospace Engineering, Xiamen University, China, yancheng.you@xmu.edu.cn*

methods are not very convenient to solve the multi-wave flowfields for the reason of input boundary conditions and algorithm procedure [15]. In addition, in order to arrange a reasonable curved-shock-system configuration and obtain a compression surface meeting the performance requirements, multi-objective optimization is usually carried out on the basis of above flowfield solution method, so that a large amount of calculation in the iterative process cannot avoid.

As above discussion, the rest of this article is organized as follows. Section 2 introduces the solving method for curved-shock multi-wave configuration flowfield and Section 3 proposes the Equal-intensity-distribution configuration and provides the flowfied calculation verification. Finally, the aerodynamic performance analysis and compression limit analysis for Equal-intensity-distribution flowfield are presented in Sections 4. The main conclusions are presented in Section 5.

2. Solving method for curved-shock multi-wave configuration flowfield

At present, the solving method of curved compression flowfield based on a given wall parameter distribution [8-11] has been successfully applied to many inverse design cases of supersonic flow field. However, how to specify a reasonable distribution of wall parameters and how to illustrate the excellent aerodynamic performance of the flow field by comparison still depend on experience or a large number of parameter optimization calculations. In addition, some problems are also existed, such as unclear optimization direction, large amount of calculation in the iterative process, and difficulty in physical interpretation. Noting that degree of design freedom in the direction of flow capture height, this paper proposes a solving method for curved-shock multi-wave configuration flowfield based on the shock intensity distribution and pressure distribution before and behind each shock. In the following, for the planar external-compression multi-wave flowfield, the proposed solving method is introduced and discussed.

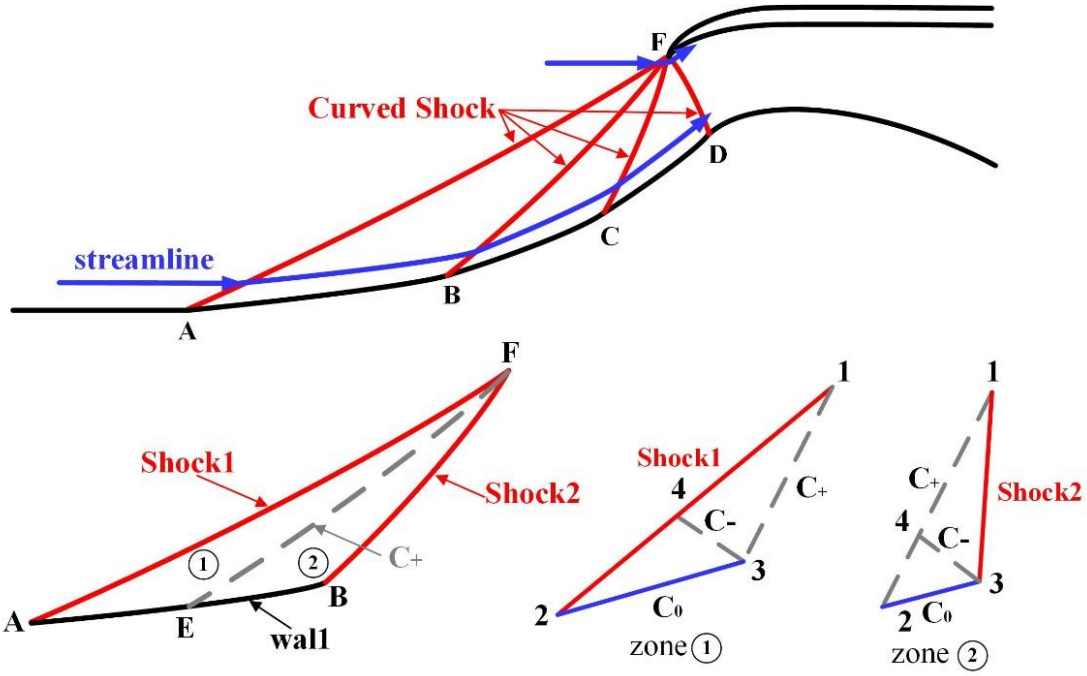

Fig 1. External-compression multi-wave curved compression flowfield and inverse method of characteristics

In the two-dimensional external-compression multi-wave curved compression flowfield shown in Figure 1, the supersonic incoming flow is decelerated to the subsonic state by passing through N ipsilateral curved shocks. The whole compression flow field is composed of N-1 inter-wave flowfield triangle region. Each flowfield triangle region can be assembled and connected by the Rankine-Hugoniot (R-H) relations, namely the pre- and post-shock relations. And for each flow field triangle region can be solved by the inverse method of characteristic. The characteristic equations and compatibility relations for the inverse method of characteristics are as follows:

$$\left(\frac{dy}{dx}\right)_0 = \frac{V_y}{V_x} \tag{1.a}$$

$$\left(\frac{dy}{dx}\right)_{\pm} = \tan\left[\delta \pm \arcsin\left(\frac{1}{Ma}\right)\right] \tag{1.b}$$

$$\rho V\, d_0 V + d_0 p = 0 \tag{1.c}$$

$$d_0 p - V_{sonic}^2\, d_0 \rho = 0 \tag{1.d}$$

$$\frac{\sqrt{Ma^2-1}}{\rho V^2} d_{\pm} p \pm d_{\pm}\delta + j\, \frac{sin\delta\, d_{\pm} x}{yMa\, cos\left[\delta \pm arcsin\left(\frac{1}{Ma}\right)\right]} = 0 \tag{1.e}$$

The subscripts in the equation mean: 0, streamline direction; ±, characteristic direction; and *j*, planar flow, $j = 0$ or axially symmetric flow $j = 1$.

For an inter-wave flowfield triangle region, it can be divided into two parts: the determination domain zone ① of the previous shock and the compression flowfield zone ② before the latter shock, where zone ① is surrounded of the initial shock AF, the front compression wall AE and the left-running characteristic EF, while zone ② is surrounded by the left-running characteristic EF, the post-compression wall EB and the shock BF. The simultaneous equations of the flow parameters at the unit points can be established by the discretization and difference process of the characteristics geometry equations and the compatibility equations.

For the calculation of the interior point in zone ①, the horizontal incoming flow and the shape of the initial shock are given as the input boundary conditions. By solving the R-H equations, the positions of point 1 and point 2 on the shock1 and their post-shock flow parameters (pressure p, density ρ, velocity V, streamwise angle δ) are known. The left-running characteristic through point 1 intersects with the streamline from point 2 at the unsolved point 3, and the reverse right-running characteristic through point 3 intersects with the initial value line 12 at point 4. The coordinate positions and flow parameters of point 3 and point 4 in the interior unit process can be solved by a few iterations of prediction and correction steps.

For the calculation of shock point at the zone ② boundary, the wave intensity distribution of the shock2 and its pre-shock pressure distribution are given, where the shock intensity is measured by the normal Mach number Ma_n. The shock emitted by point 1 intersects with the streamline emitted by point 2 at unsolved shock point 3, and the right-running characteristic emitted by point 3 intersects with the left-running characteristic 12 at point 4, thus forming the solution unit of shock point. It is known that the coordinate position of point 1 and point 2 (x_1, y_1, x_2, y_2) and their flow parameters (p_1, ρ_1, V_1, δ_1, p_2, ρ_2, V_2, δ_2). The shock intensity at point 1 and point 3 (Ma_{n1}, Ma_{n3}) and the pressure p_3 at point 3 are also known. Firstly, the coordinate positions of point 3 and point 4 can be estimated by the difference geometric equations (2a-d), and the flow parameters (p_4, ρ_4, V_4, δ_4) of point 4 can be estimated by linear interpolation on the left-running characteristic 12.

$$y_1 - y_3 = \tan(\delta_1 + \beta_1)\,(x_1 - x_3) \tag{2.a}$$

$$y_3 - y_2 = \tan(\delta_2)\,(x_3 - x_2) \tag{2.b}$$

$$y_4 - y_3 = \tan(((\delta_1 - \mu_1) + (\delta_2 - \mu_2))/2)\,(x_4 - x_3) \tag{2.c}$$

$$y_4 - y_1 = (y_1 - y_2)/(x_1 - x_2)(x_4 - x_1) \tag{2.d}$$

Where β denotes the shock angle $\beta = \arcsin\,(Ma_n/(V/\sqrt{\gamma p/\rho}))$, μ is the Mach angle $\mu = \arcsin\,(1/Ma)$. Since the pressure p_3 of point 3 is given, other predicted flow parameters (ρ_3, V_3, δ_3) of point 3 can be solved by the differential form of compatible equations (3a-c).

$$\rho_2 V_2 (V_3 - V_2) + (p_3 - p_2) = 0 \tag{3.a}$$

$$(p_3 - p_2) - \gamma p_2/\rho_2 (\rho_3 - \rho_2) = 0 \tag{3.b}$$

$$\frac{\sqrt{Ma_4^2-1}}{\rho_4 V_4^2}(p_3 - p_4) - (\delta_3 - \delta_4) + j\,\frac{\sin(\delta_4)(x_3 - x_4)}{y_4 Ma_4 \cos(\delta_4 - \mu_4)} = 0 \tag{3.c}$$

At this time, The predicted shock wave angle at point 3

$$\beta_3 = \arcsin\left(Ma_{n3}/(V_3/\sqrt{\gamma p_3/\rho_3})\right) \tag{3.d}$$

Based on the predicted streamwise angles, Mach angles at points 3 and 4 and the shock angle β_3, the geometric equations (2a-c) are further corrected as

$$y_1 - y_3 = \tan((\delta_1 + \beta_1 + \delta_3 + \beta_3)/2)\,(x_1 - x_3) \tag{4.a}$$

$$y_3 - y_2 = \tan((\delta_2 + \delta_3)/2)\,(x_3 - x_2) \tag{4.b}$$

$$y_4 - y_3 = \tan(((\delta_4 - \mu_4) + (\delta_3 - \mu_3))/2)\,(x_4 - x_3) \tag{4.c}$$

The corrected coordinates of point 3 and point 4 and the flow parameters at point 4 are obtained again. At the same time, the compatible equations (3a-c) are also corrected as

$$\overline{\rho}_{23}\overline{V}_{23}(V_3 - V_2) + (p_3 - p_2) = 0 \tag{5.a}$$

$$(p_3 - p_2) - \gamma\overline{p}_{23}/\overline{\rho}_{23}(\rho_3 - \rho_2) = 0 \tag{5.b}$$

$$\frac{\sqrt{\overline{Ma}_{34}^2 - 1}}{\overline{\rho}_{34}\overline{V}_{34}^2}(p_3 - p_4) - (\delta_3 - \delta_4) + j\frac{\sin(\overline{\delta}_{34})(x_3 - x_4)}{\overline{y}_{34}\overline{Ma}_{34}\cos(\overline{\delta}_{34} - \overline{\mu}_{34})} = 0 \tag{5.c}$$

The superscript ' - ' represents the average value of the predicted parameters of two discrete points, and the subscript represents the number of the two discrete points. By combining the equations (5a-c), the flow parameters (ρ_3, V_3, δ_3) of point 3 after correction can be obtained, and the shock angle β_3 of point 3 can be further obtained. In this way, the convergence results of the coordinates, density, velocity, streamwise angle and shock angle of shock point 3 can be obtained after a few iterations of prediction and correction steps. Once the solution process of shock point 3 is completed, the remaining interior points in zone ② can be calculated along the left-running characteristic through point 3, which is the same as that in zone ①.

From the above solution process of the flowfield triangle between waves, it can be seen that under specific incoming flow, the input boundary conditions for solving the curved-compression flowfield of the external-compression multi-wave system include:

- 1 the shape of the first shock, named initial shock in this paper, (intensity distribution) is given.
- 2 The intensity distributions of the following shock waves are given respectively.
- 3 The pressure distributions before the following shock waves are given respectively.

In previous researches, in order to achieve the inverse design of multi-stage compression flowfield, there are two ways to solve the zone ②: One is to extend the shock AF, expand its shock determination domain, and then specify the shock shape BF of the next stage compression in this determination domain; the other is to specify the parameter distributions of the post-compression wall EB, and thus calculating the compression flow field downstream of the left-running characteristic EF, for example, the inverse design methods based on given wall pressure distribution or wall Mach number distribution. In general, the idea of both is first expanding the post-wave flowfield region of the previous shock, then specifying the latter shock wave and complete its post-wave flow field calculation, and finally intercepting the excess flow field part. Compared with the previous methods, the solving method for the multi-wave curved-compression flowfield adopted in this paper only changes the input of boundary conditions, but avoids the process of flow field expansion calculation and truncation. More importantly, by directly specifying the pressure distribution before each shock wave and the intensity distribution of the shock itself, it is not only concerned with the compression process of a streamline attached to the wall, but also describes the whole process of airflow compression at the whole capture height. From this physical point of view, based on the proposed solving method for flowfield inverse design, the study of multi-wave curved shock arrangement problem can be carried out conveniently.

3. Equal-intensity-distribution configuration

According to the above discussion on the solving method of multi-wave curved-compression flowfield, a specific flowfield solution can be determined by giving the pressure distribution before each shock and the intensity distribution of the shock itself. However, due to the large degree of freedom of the input distribution, the guiding value for the study of curved shocks arrangement is still not clear. In the following, focusing on the equal-intensity-distribution configuration, the aerodynamic performances of total pressure recovery and compression efficiency of the flow field are analyzed.

3.1. Equal intensity distribution assumption

According to Oswatitsch 's optimal wave system theory, the airflow is decelerated and pressurized by N-1 oblique shock wave and 1 normal shock wave. If the normal Mach numbers of N-1 oblique shocks are equal and the Mach number before the terminal normal shock is about 0.94 times of the normal Mach number of oblique shock wave ($1.5 \le Ma_\infty \le 5$), the total pressure recovery of the flow field is the highest [1]. This conclusion is extended to the case of curved-shock wave system, and the following assumptions of equal intensity distribution for shocks arrangement are given as:

- 1 Each curved shock converges at a focus, at which is only affected by shock compression;
- 2 The pressure behind the terminal shock is the same, and the flow field is isobaric compression;
- 3 The intensity of each discrete shock segment that arbitrary streamline passes through is equal; (Except the terminal shock, the pre-shock Mach number of the terminal shock is configured as 0.94 times that of first several shock waves)
- 4 The pressure ratio of the isentropic zone between waves that arbitrary streamline passes through is equal;

By introducing above equal intensity distribution assumption, the calculation steps of the multi-wave curved-shock flowfield of equal-intensity-distribution configuration are as follows :

(1) Given the incoming flow parameters (including pressure p_0, density ρ_0, velocity v_0, streamwise angle δ_0, Mach number Ma_∞), it is advisable to set the coordinate of shock convergence focus at point (0, 1). Since the shock focus is only compressed by the shock wave, in order to obtain the maximum total pressure recovery at this point, the intensity of each curved shock at this focus can be arranged according to the Oswatitsch optimal wave system theory, and the pressure p_N behind the terminal shock can be obtained.

(2) Given the first initial curved shock function, the initial shock satisfies the shock angle limit at the focus, and the intensity of the shock gradually weakens from the end of the focus to the other end of the compression surface. The intensity distribution of initial shock and the corresponding shock pressure ratio distribution are obtained, and the shock pressure ratio at any point on it is expressed by R_s.

(3) Arbitrary streamline within the capture height will be compressed through N shocks and N-1 isentropic regions. According to the assumption of equal intensity distribution, the pressure ratio of each discrete shock segment that the streamline passes through is equal (except the pressure ratio of the terminal shock R_{sN}), namely $R_{s1} = R_{s2} = \cdots = R_{s(N-1)} = R_s$, the pressure ratio of each isentropic zone that the streamline passes through is equal, namely $R_{ise1} = R_{ise2} = \cdots = R_{ise(N-1)} = R_{ise}$. Since the pressure behind the terminal shock is equal, the pressure ratio in the isentropic region can be calculated as

$$R_{ise} = \sqrt[(N-1)]{\frac{p_N / p_0}{R_s^{(N-1)} R_{sN}}} \tag{6}$$

Post-shock pressure in the ith discrete shock segment

$$p_{i\_behind} = p_0 R_s^i R_{ise}^{(i-1)} \tag{7}$$

Pre-shock pressure in the (i+1)th discrete shock segment

$$p_{i+1\_front} = p_0 R_s^i R_{ise}^i \tag{8}$$

Considering the whole capture height, the pressure distribution before and behind each curved shock can be obtained.

(4) The inverse method of characteristics is used to calculate each inter-wave flowfield triangle, including the shock determination domain zone ① and the post-compression surface flowfield zone ②, until the calculation of N-1 inter-wave flowfield triangles is completed. The specific process is shown in Figure 2

Overall, due to the assumption that the input boundary conditions 2, 3 are associated with boundary condition 1, the multi-wave flow field is actually determined by the initial shock.

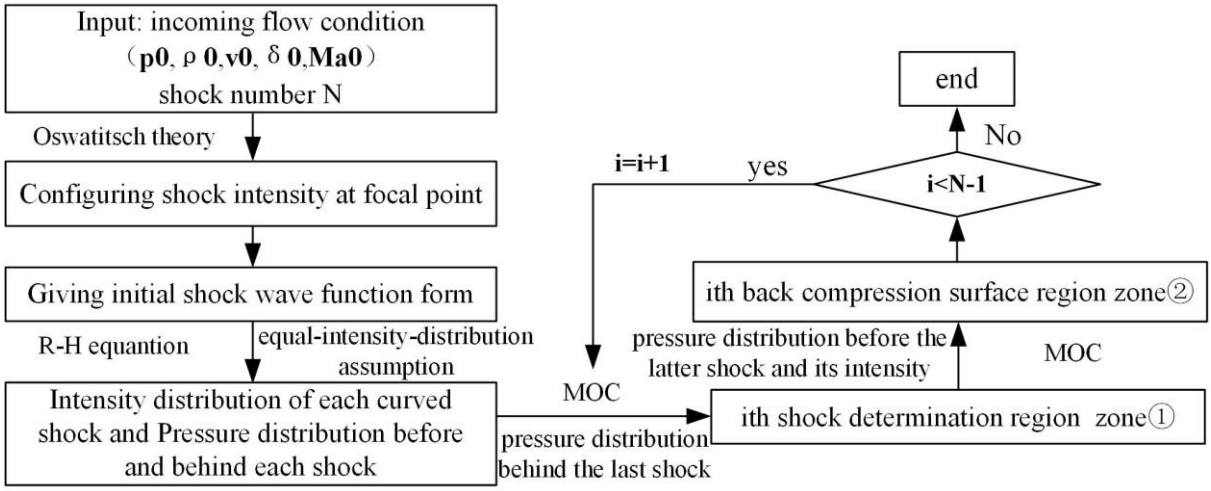

Fig 2. Calculation process for equal-intensity-distribution flowfield

3.2. Equal-intensity-distribution flowfield solution verification

In order to verify the accuracy of the solving method, a comparative study with the CFD inviscid simulation results was carried out. In the verification case, the Mach number of incoming flow is set to Ma3.0, and the initial shock equation is given, which could be a quadratic function $y = 0.0434x^2 + 0.5406x + 1$. The three-stage compression wall of the equal-intensity-distribution flowfield is obtained by the inverse method of characteristic. The computational domain of CFD numerical simulation of two-dimensional planar flow is discretized by structured grids. And the total number of grids is 30,000, and the grid resolution is sufficient to obtain a convergence result. The incoming flow is assumed as an ideal gas, the freestream boundary condition adopts the pressure far field, the outlet adopts the pressure outlet boundary, and the outlet pressure is 20.8 times than the freestream pressure, and a slip condition is applied to the wall boundary. The inviscid flux is calculated by the Roe-FDS algorithm, and the governing equation is solved by the second-order upwind discretization method with fully implicit scheme. The calculation convergence criterion is that the residuals of the continuous equation, the momentum equation, and the energy equation are reduced to less than 10^{-3} or the residuals of the continuous iteration are no longer reduced.

The computational domain, boundary conditions and pressure field of CFD numerical simulation are shown in Figure 3 (a). The flow field results calculated by the inverse method of characteristics are also embedded in Figure 3 (a). The shocks and isoparametric curves of the CFD and the MOC results are represented by black solid curves and red dotted curves, respectively. It can be seen that the captured shock structures and pressure contour are in good agreement. Three streamlines are extracted from the inflow capture height Y = 0.35, 0.7 and 0.95 respectively. Their pressure changes along the path are shown in Figure 3 (b). The vertical step of pressure is shock compression, while the relatively slow

increase along the flow direction is isentropic compression. Ignoring the shock thickness in CFD flow field, the streamline pressure-rise distributions of the inverse MOC are in good agreement with the CFD calculation results. For the compression processes of the three streamlines, under the same pressure ratio behind the terminal shock, the proportion of shock compression and isentropic compression of different streamlines in the flow field is different, and the total pressure loss is different. For the streamline 1, the contribution of the shock compression is large and that of the isentropic compression is little, while the isentropic compression of streamline 2 and 3 is larger, and the intensities of the shocks that the streamline 2 and 3 pass through are weaker. The shock wave and the isentropic compression wave have a considerable contribution to the final compression state. Behind the terminal shock, in the case of non-viscous, the total pressure recovery of the streamline near the shocks focus is low, while the total pressure recovery of the streamline near the compression wall is high.

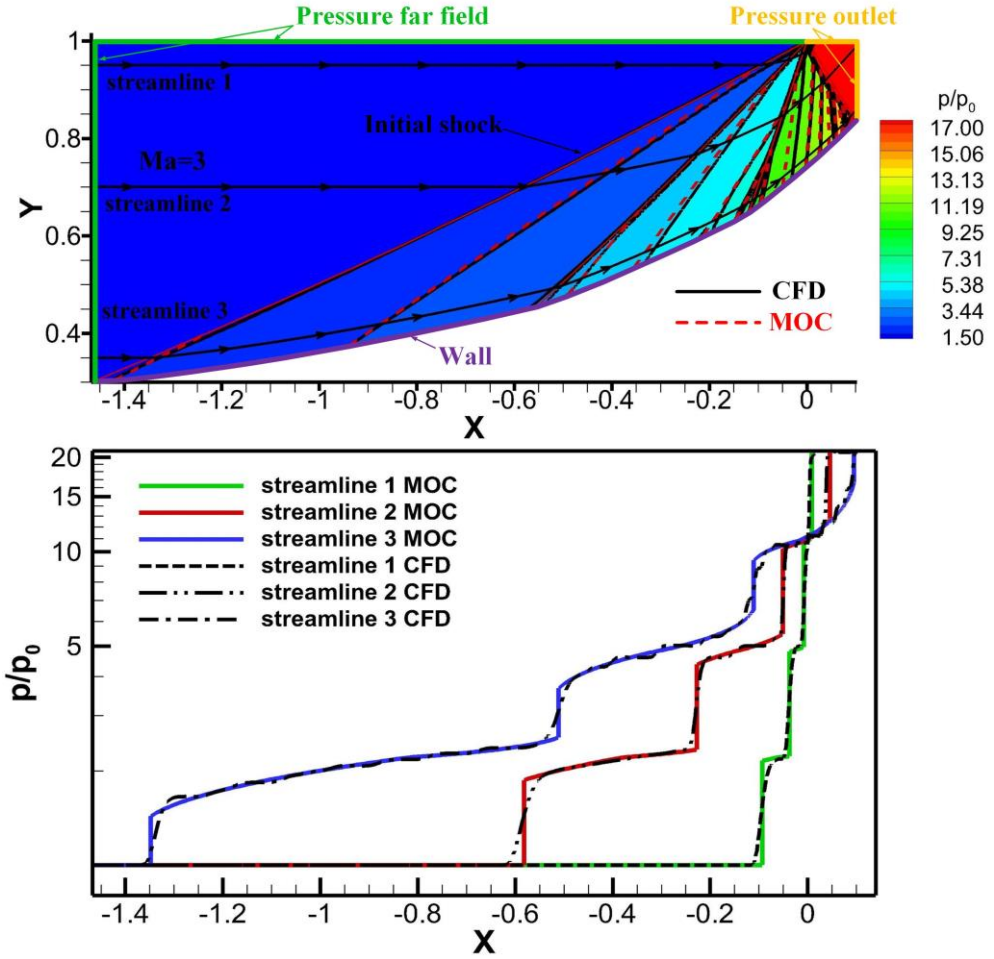

Fig 3. Four-wave system three-stage curved-shock compression flowfield contour and streamline pressure-rise distribution verification

4. Aerodynamic performance analysis for Equal-intensity-distribution flowfield

4.1. Planar flows

For the curved-shock wave system, due to the existence of isentropic compression component, the greater the contribution of isentropic compression, the higher the total pressure recovery in theory. If the total pressure recovery is only the optimization goal without other constraints, the flow field may tend to be completely isentropic compression configuration. Considering that the length of the surface of the isentropic compression configuration is too long, which may be contrary to the advantage of the high compression efficiency of the curved compression configuration, the compression efficiency index should be introduced as another optimization target reference when configuring the curved-shock wave system.

The surface compression efficiency ratio *Ks* is defined as:

$$K_s = \frac{\pi \cdot \sigma}{S \cdot \varphi} \tag{9}$$

where π and σ are the pressure ratio and the total pressure recovery behind the terminal shock, respectively. $\pi \cdot \sigma$ can be understood as the pressure rise efficiency, S is the dimensionless area of compression surface, and φ is the flow coefficient. As a new parameter to evaluate the compression efficiency of the compression surface, there are few quantitative studies on this parameter.

The arc equation maybe be taken as the functional form of the initial curved shock so that the shock curvature can be express by a value.

$$y = -\sqrt{-x^2 + 2(1-a) * \tan(\beta_1)\, x + (1-a)^2} + a \tag{10}$$

Where β_1 is the shock angle of the initial shock wave at the focus. When the parameter a tends to be infinite, the equation tends to be linear. As the parameter a decreases, the curvature of the initial shock gradually increases. The equation guarantees that the initial shock passes through the convergence focus (0, 1). The intersection of the shock curve and the x-axis is the leading edge of the compression surface. The compression surface length L is defined as the horizontal distance from the leading edge to the convergence focus. The height of the convergence focus is recorded as H, and the spanwise length of the compression surface is taken as the circumference ratio pi.

In incoming flow of Ma 3.0 and under the condition of full capture, the variations of total pressure recovery (left) and surface compression efficiency ratio (right) of equal-intensity-distribution flowfields under different number of shocks are shown in Figure 4. For the two-, three- or four-wave system flowfields, the left end of the total pressure recovery curve begins with the maximum solution of the total pressure recovery in the straight shock system. With the increase of the initial shock curvature, the dimensionless length of the compression surface L/H increases continuously, and the total pressure recovery also increases until the right end of the performance curve, where the compression limit is reached. Comparing the right end of the two-wave curve with the left end of the three-wave curve, under the same compression length, the total pressure recovery of the two-wave flowfield is higher than that of the three-wave case, and the same results are obtained for the three-wave and the four-wave flowfield. It is suggested that enhancing the curved compression characteristics of the initial shock wave, rather than adding one or two shock waves, could be possible to achieve a total pressure recovery equivalent to or even better than that of the straight shock system, so as to simplify the flowfield wave system.

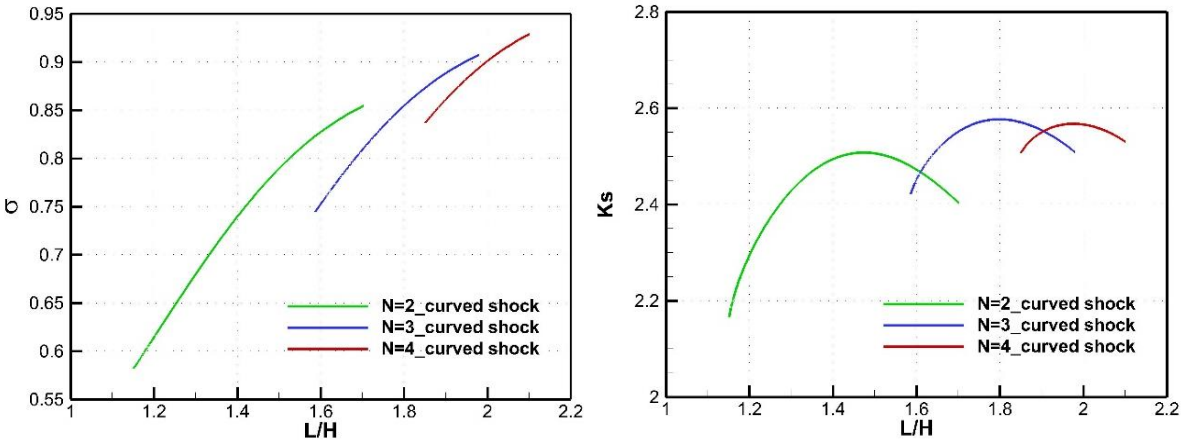

Fig 4. Performance curves of total pressure recovery and compression efficiency under different number of shocks in incoming flow of Ma 3.0

Beginning from the left end of *Ks* curves, the total pressure recovery increases rapidly and becomes the dominant factor to improve the compression efficiency. With the further increase of the shock curvature, the total pressure recovery growth slows down, while the compression length increases rapidly, which leads to the gradual decrease of the compression efficiency. So there is always a maximum value of the surface pressure efficiency ratio *Ks*. Therefore, limiting the curvature of the

initial shock within a certain range could improve the compression efficiency, achieving the reasonable allocation of shock compression and isentropic compression.

Figure 5 shows the Ma number contours of equal-intensity-distribution flowfields corresponding to the solutions of maximum compression efficiency and compression limit in Figure 4.

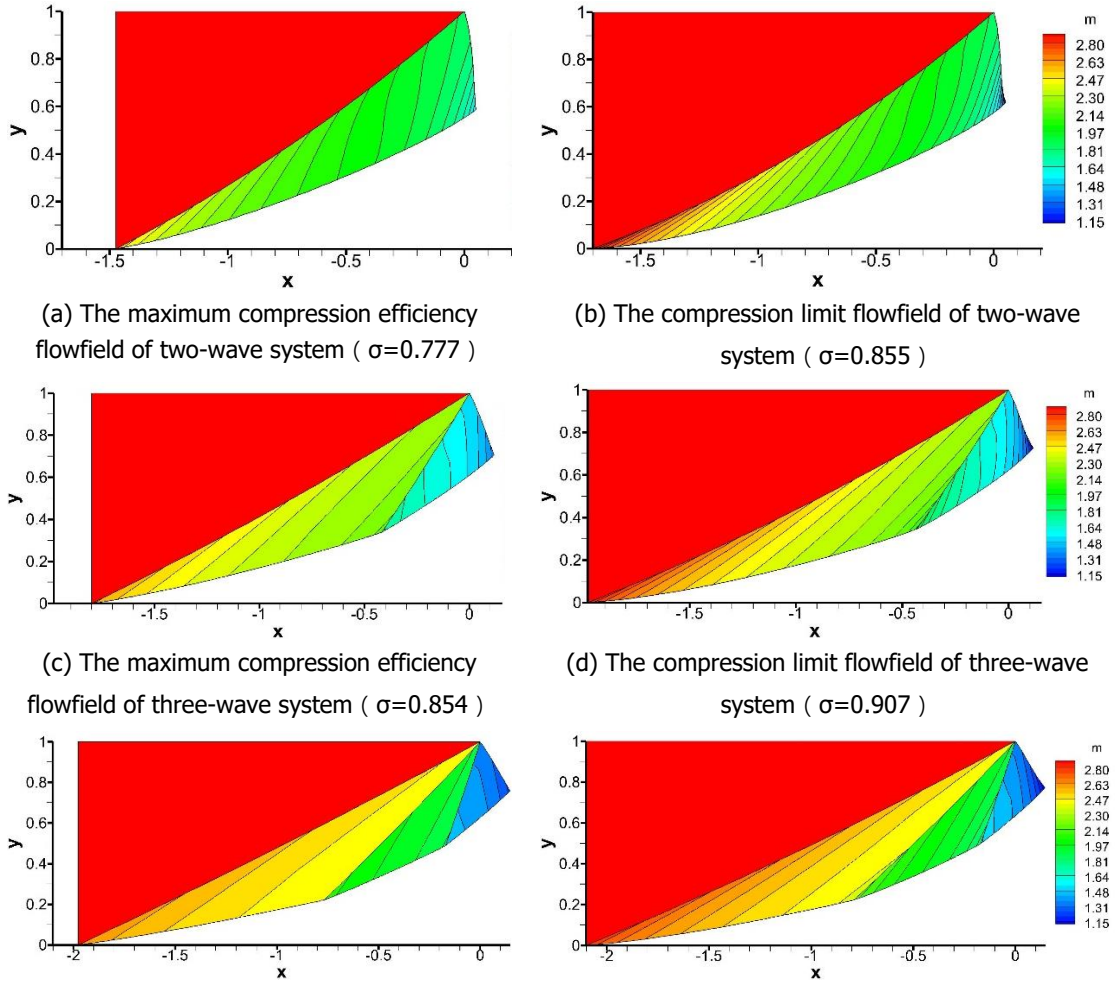

(a) The maximum compression efficiency flowfield of two-wave system (σ=0.777)

(b) The compression limit flowfield of two-wave system (σ=0.855)

(c) The maximum compression efficiency flowfield of three-wave system (σ=0.854)

(d) The compression limit flowfield of three-wave system (σ=0.907)

(e) The maximum compression efficiency flowfield of four-wave system (σ=0.893)

(f) The compression limit flowfield of four-wave system (σ=0.929)

Fig 5. Maximum compression efficiency and compression limit of equal-intensity-distribution flowfields under different shock numbers in incoming flow of Ma3.0

4.2. Axisymmetric flows

The above discussions all have corresponding axisymmetric cases. The x-axis is the symmetry axis, the radial height of the shocks convergence focus is H, and the height of the central body is h, which is also the radial height of the compression leading edge, (h < H). If the height of the central body tends to 0, the solution tends to the multi-stage external-cone flowfield, and the capture area is a circular area with a radius of H, whose value is equal to the capture area of the above planar flow. This paper will ignore the singularity error in solving the cone-top flow field.

Figure 6 shows the counterpart of Figure 4 for the external-cone axisymmetric flowfields. The left end of the total pressure recovery curve represents the flow field solution when the initial shock is a straight cone. Although the latter shocks are not straight shocks, for streamlines with different radial heights, the compression process through each shock and each isentropic region is the same, so the total pressure recovery is equal to that of the straight-shock wave system in the planar flow. With the increase of the initial shock curvature, the total pressure recovery of the streamline near the symmetry axis increases continuously. Compared with the planar flow, the total pressure recovery of the

axisymmetric flow field is lower and the compression efficiency is higher with the same function of initial shock (or the same length of compression surface). This is due to the low proportion of mass flow rate with high total pressure recovery near the symmetry axis and the small area of the curved-cone compression surface. The compression limit of the axisymmetric flow field is also the solution of the maximum compression efficiency. The compression limit contours of external-cone axisymmetric flowfields are presented in Figure 7.

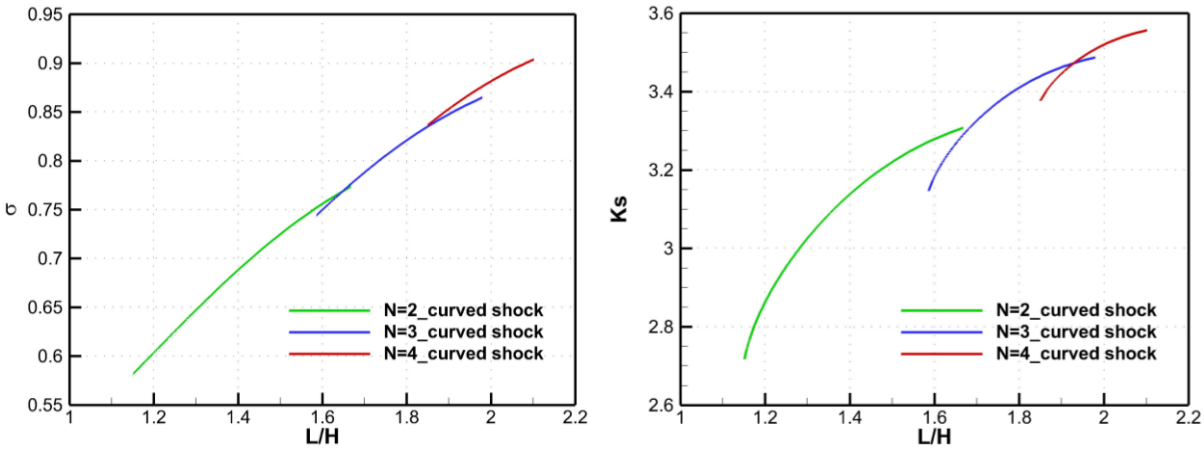

Fig 6. Counterpart of Fig. 4 for the external-cone axisymmetric flowfields

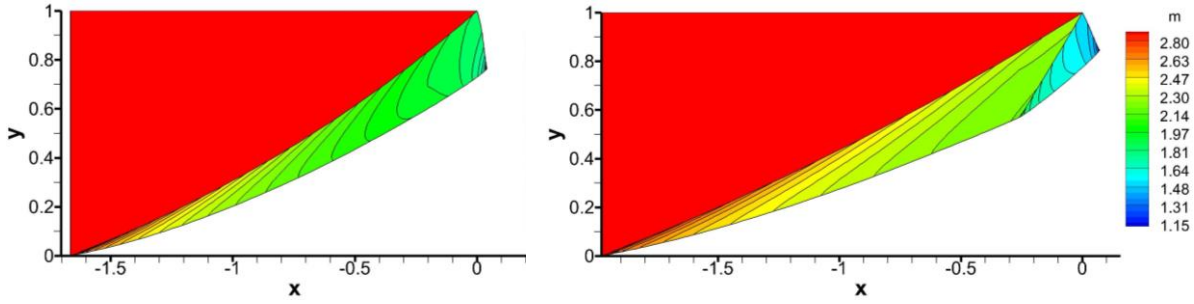

(a) The compression limit flowfield of two-wave system (σ=0.774)

(b) The compression limit flowfield of three-wave system (σ=0.865)

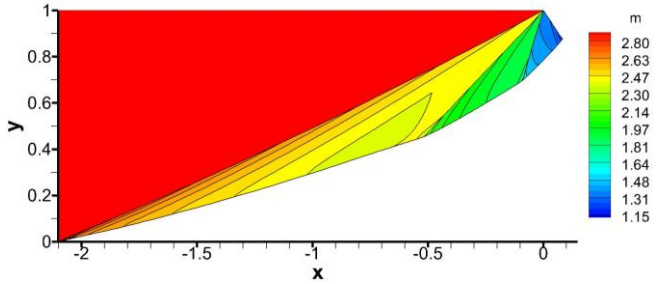

(c) The compression limit flowfield of four-wave system (σ=0.904)

Fig 7. Compression limit of external-cone axisymmetric flowfields with equal-intensity-distribution configuration under different shock numbers in incoming flow of Ma3.0

Under different the central body radius, performance curves of axisymmetric flowfields are shown in Figure 8. The compression area S in equation (9) is calculated under the same capture area of circumference ratio pi. The influence of the central body radius could be concluded as the fact that the larger the radius of the central body, the more the flowfield characteristics tend to be two-dimensional planar flow.

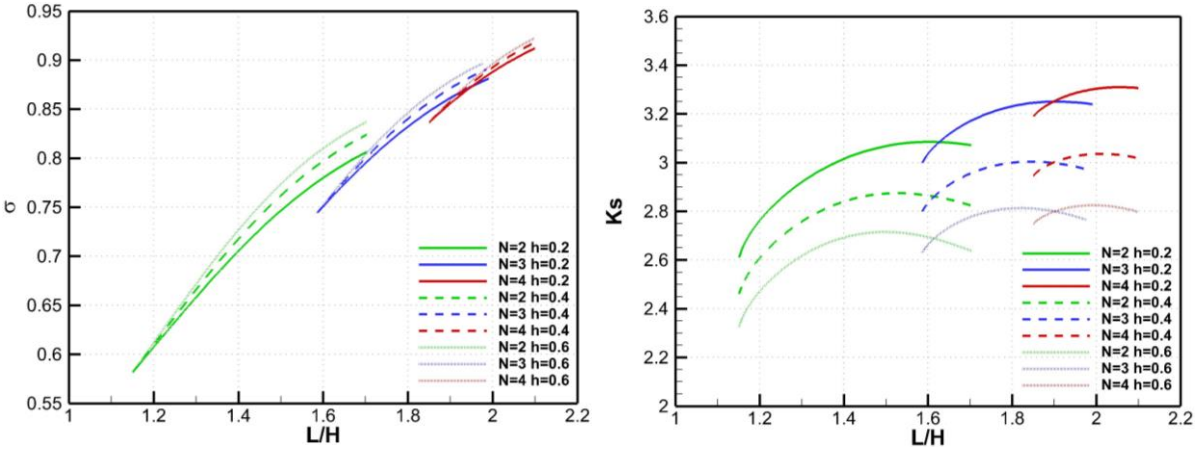

Fig 8. Performance curves of axisymmetric flowfields with equal-intensity-distribution configuration under different height of central body

4.3. Initial shock effect analysis and curved compression limit

Due to the assumption of equal intensity distribution, the flow field is determined by the initial shock. In the following, the influence of different initial shock shapes on the total pressure performance / compression efficiency is analyzed, and it is discussed that the curved compression limit that different equations of initial shock could reach.

The shape of the initial shock discussed in this paper is limited to a monotonically increasing convex function, that is, the intensity of the shock gradually increases with the increase of the capture height. The equation can be expressed as $y = xg(x) + 1$, and satisfying $g(0) = \tan(\beta_1)$ can guarantee the shock angle limit of the initial shock at the focus. Let $g(x)$ be $ax + \tan(\beta_1)$ and $-a\sqrt{-x} + \tan(\beta_1)$, respectively. The following equations (1) and (2) are obtained, including the arc equation (3), having:

(1) Quadratic function : $y = x(ax + \tan(\beta_1)) + 1$

(2) 3/2 power polynomial : $y = x\left(-a\sqrt{-x} + \tan(\beta_1)\right) + 1$

(3) Arc equation : $y = -\sqrt{-x^2 + 2(1-a) * \tan(\beta_1)\, x + (1-a)^2} + a$

The curvature variation of the three shock shapes are different but representative. As the capture height increases, the curvature of equation (1) gradually decreases, the curvature of equation (2) gradually increases, and the curvature of equation (3) remains unchanged.

The flow field of the two-wave system is analyzed. As shown in Figure 9, when the compression length L/H is short, the shock curvature is not large, and the performance difference caused by the three shock shapes is very little. As the initial shock curvature increases, the compression length of the flow field continues to increase, and the performance curves corresponding to the three shock shapes begin to bifurcate gradually. When the initial shock adopts Equation (2), the compression limit which could be achieved has the longest compression length and the highest total pressure recovery, but the lowest compression efficiency. When the initial shocks are equations (3) and (1), respectively, the compression length and the total pressure recovery of the compression limit decrease in turn, and the compression efficiency increases in turn.

Under a specific Mach number, the enhance of flowfield curved-compression characteristics will eventually be limited by the following:

1 The minimum shock angle of each curved shock wave is greater than the Mach angle ;

2 The wall-attached streamline passing through the minimum shock angle can achieve the specified pressure behind the terminal shock by supplementing the isentropic compression.

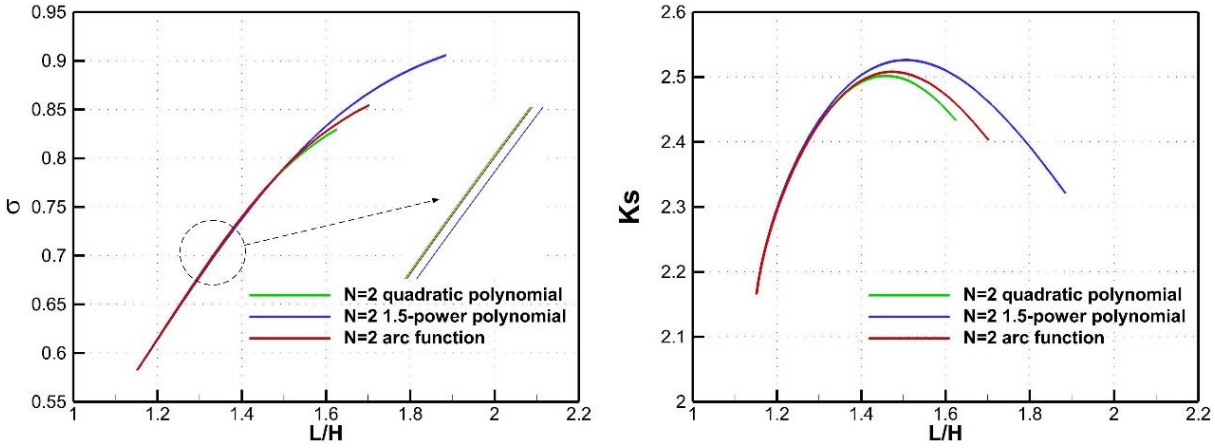

Fig 9. Comparison of total pressure recovery and compression efficiency under different initial shock shapes in two-wave system

In view of the above two limitations, it could be analyzed that the influence of different shock curvature distribution on the limit state of curved-compression flowfield. On the one hand, compared with the focus end of the initial shock, the smaller the local curvature of the shock at the end of the compression surface, the greater the curved-compression limit that the flow field could reach, and the more the flow field tends to be isentropic compression, but the length of the compression surface is larger and the pressure at the end of the compression surface rises sharply. On the other hand, the greater the local curvature of the initial shock at the end of the compression surface, the smaller the curved-compression limit that the flow field can reach, and the more the flow field tends to shock compression. This is because the weaker end of the shock coincides with the larger end of the shock curvature. And the shock compression amount of the wall-attached streamline decreases rapidly, however, the isentropic compression process is limited by the compression state of the previous layer of streamline, in other words, the limitation of the characteristic equations and compatibility relations for the method of characteristics, which results in the inability of the isentropic compression amount to compensate for the reduced shock compression amount, thus failing to reach the specified post-shock pressure of the terminal shock.

5. Conclusions

In this paper, based on the computational principle of the inverse method of characteristic, an inverse design method that can specify the compression process of the two-dimensional/axisymmetric captured flow tube is developed for the external-compression multi-wave flowfield of curved surface compression. On this basis, it is proposed that a kind of configuration for curved shock system with the same intensity distribution in the capture height direction, and named Equal-Intensity-Distribution configuration. The multi-wave flow field with Equal-Intensity-Distribution configuration is actually determined by the initial shock.

An index parameter Ks named surface compression efficiency ratio is introduced to measure the performance of the equal-intensity-distribution flowfield. The both characteristics of the total pressure recovery and the compression efficiency in the cases of different shock numbers are emphatically studied. The results show that enhancing the curved compression characteristics of the initial shock, rather than adding one or two shock waves, could be possible to achieve a total pressure recovery equivalent to or even better than that of the straight shock system, so as to simplify the flowfield wave system. In addition, limiting the curvature of the initial shock within a certain range could improve the compression efficiency, achieving the reasonable allocation of shock compression and isentropic compression.

In addition, the compression limit of curved shock system is discussed when the initial shock wave is given in different function forms. For the initial shock wave in the form of convex function, on the one hand, compared with one end of the focused shocks, the smaller the shock curvature at the other end away from the shock focal point, the higher total pressure recovery that the compression limit could

reach, and the more the flow field tends to be isentropic compression, but the compression surface is longer, the compression efficiency could be lower. On the other hand, the greater the local curvature of the initial shock at the end of the compression surface, the smaller the curved-compression limit that the flow field can reach, and the more the flow field tends to shock compression.

References

1. Oswatitsch, K.: Pressure Recovery in Missiles with Reaction Propulsion at High Supersonic Speeds. NACA TM-1140 (1947).
2. James, F. Connors, Rudolph, C. Meyer.: Design Criteria for Axisymmetric and Two-Dimensional Supersonic Inlets and Exits. NACA TN-3589 (1956).
3. Henderson L F.: Maximum Total Pressure Recovery across a System of n Shock Waves. AIAA Journal, 2(6), 1138-1140 (1964).
4. Zhang Kunyuan，Meier G E A. Using R. C. Method to Study Optimum Compression Surface under Non-Uniform 2-D Supersonic Flow Condition. AIAA 94-1838
5. Emanuel G. Supersonic Compressive Ramp without Laminar Boundary-Layer Separation. *AIAA Journal*, 22(1): 29-34 (1984)
6. Pan Jin, Zhang Kunyuan.: Experimental and Numerical Investigation of a Curved Compression System Designed on Constant Pressure Gradient. *AIAA* 2009- 5270
7. Nan Xiangjun，Zhang Kunyuan. Numerical and Experimental Investigation on Hypersonic Inward Turning Inlets with Basic Flowfield Using Arc Tangent Curve Law of Pressure Rise. *AIAA* 2011-2270
8. Li, Yongzhou, Zhang Kunyuan.: Design of hypersonic inward turning inlets with controllable Mach number distribution. 48th AIAA/ASME/SAE/ASEE Joint Propulsion Conference & Exhibit. (2012)
9. Zhang Lin, Zhang Kunyuan. Numerical Investigation of Hypersonic Curved Shock Two-Dimensional Inlet Designed on the Wall Constant Mach Number Gradient. *AIAA* 2012-4065.
10. Nan X J, Zhang K Y. Numerical and Experimental Investigation on Hypersonic Inward Turning Inlets with Basic Flowfield Using Arc Tangent Curve Law of Pressure Rise. *AIAA* 2011-2270
11. Li Yiqing，Han Weiqiang，Teng Jian.: An Innovative Integration Concept for Forebody and Two-Dimensional Hypersonic Inlet with Controllable Wall Pressure Distribution. *AIAA* 2015-3592.
12. Fang X J, Zhang K Y.: Inverse Design of Supersonic Internal Flow Path Based on Given Outflow Velocity Profile. AIAA 2012-4064.
13. YOU, Y.C. & LIANG, D.W.: Design concept of three-dimensional section controllable internal waverider hypersonic inlet. *Sci. China Ser.* E *Technol. Sci.* 52, 2017–2028 (2009)
14. Zhang L, Zhang K Y, Wang L.: Application Study of the Curved Surface Compression System in Three-Dimensional Sidewall Compression Inlet. *AIAA* 2014- 2840
15. Zhang Kunyuan.: Research Progress of Hypersonic Inlet Inverse Design Based on Curved Shock Compression System. AIAA 2015-3647